Hepatic Disposal of Advanced Glycation End Products During Maturation and Aging

Dmitri Svistounov [a]*, Ana Oteiza [a], Svetlana N. Zykova [b], Karen Kristine Sørensen [a], Peter McCourt [a], Andrew McLachlan [c], Robert S. McCuskey [d], Bård Smedsrød [a].

[a]Department of Medical Biology, University of Tromsø, Tromsø, Norway

[b]Department of Nephrology, University Hospital of Northern Norway, Tromsø, Norway

[c]Faculty of Pharmacy, University of Sydney, Australia

[d]University of Arizona, Tucson, Arizona, USA

*** Corresponding author at:** Department of Medical Biology, University of Tromsø, Tromsø, Norway

Tel.: +47 45063451; +47 77656020 E-mail address: d.svistounov@gmail.com

Abbreviations: Advanced glycation end products (AGEs); AGE degradation products (AGE-DPs); liver sinusoidal endothelial cells (LSECs); Kupffer cells (KCs); parenchymal cells (PCs); Akaike's Information Criterion (AIC); Area under the curve (AUC); Molecular weight (MW)

ABSTRACT

Aging is characterized by progressive loss of functions and accumulation of metabolic by-products, including advanced glycation end products (AGEs), which are observed in

several pathological conditions. A number of waste macromolecules, including AGEs are taken up from the circulation by endocytosis mainly in liver sinusoidal endothelial cells (LSECs) and Kupffer cells (KCs). However, AGEs still accumulate in tissues with age. The aim of the present study was to determine whether the efficiency of LSECs and KCs for disposal of AGEs changes through aging.

Results: After intravenous administration of ^{14}C-AGE-albumin in pre-pubertal, young adult, middle aged and old mice, more than 90% of total recovered ^{14}C-AGE was liver associated, irrespective of age. LSECs and KCs represented the main site of uptake. A fraction of the ^{14}C-AGE degradation products (^{14}C-AGE-DPs) was stored for months in the lysosomes of these cells after uptake. The overall rate of ^{14}C-AGE-DPs removal from the liver was markedly faster in pre-pubertal than in all post-pubertal age groups. The ability to dispose of ^{14}C-AGE-DPs decreased to similar extents after puberty in LSECs and KCs. A fast early removal phase was characteristic for all age groups except the old group, where this phase was absent.

Conclusions: Removal of AGE-DPs from the liver scavenger cells is a very slow process that changes with age. The ability of these cells to dispose of AGEs declines after puberty. Decreased AGE removal efficiency early in life may lead to AGE accumulation.

Highlights: ▶ ^{14}C-AGE allows long term tracking of intracellular metabolism of the AGE-adduct ▶ AGE degradation products (AGE-DPs) accumulate in lysosomes of liver scavenger cells ▶ Liver scavenger cell discharge of AGE-DPs decreases after puberty

Keywords: aging; scavenger cell; liver; lysosome; AGE accumulation; AGE disposal

1. Introduction

Advanced glycation end-products (AGEs) are heterogeneous compounds formed by non-enzymatic, irreversible glycosylation/glycoxydation of proteins (Baynes and Thorpe, 1999; Horie et al., 1997; Ling et al., 1998). This modification alters protein characteristics and renders them resistant to proteolysis (Miyata et al., 1997; Sell et al., 1996). Accumulation of AGEs in tissues is harmful (Baynes and Thorpe, 1999; Makita et al., 1994), observed in several pathological conditions (Hammes et al., 1999; Horie et al., 1997; Niwa, 2006), and is thought to result from chronic hyperglycemia, and increased oxidative and carbonyl stress (Baynes and Thorpe, 1999; Makita et al., 1994).

Because AGEs are also formed as by-products of normal metabolic processes, aging is associated with higher appearance of AGEs in various tissues including liver (Baynes and Thorpe, 1999; Dunn et al., 1991; Hammes et al., 1999; Horie et al., 1997; Ling et al., 1998; Schleicher et al., 1997). In humans and other mammals the rate of AGE accumulation correlates inversely with species longevity (Sell et al., 1996). AGEs accumulate faster in shorter-lived compared with longer-lived mouse strains (Sell and Monnier, 1997). However, it is not clear whether AGE accumulation is a cause of aging or a consequence of age-related decline in their elimination, or both.

Intravenously administered AGE modified bovine serum albumin (AGE-BSA) is rapidly removed from the circulation via scavenger receptor-mediated endocytosis in the liver scavenger cells, i.e. liver sinusoidal endothelial cells (LSECs) and Kupffer cells (KCs) (Smedsrod et al., 1997). However, AGEs still accumulate in tissues with age. The aim of the present study was to determine whether the effiency of liver scavenger cells for disposal of accumulated AGE wastes changes through maturation and aging. The liver

handling of AGEs was examined in four age groups of C57BL/6 mice; prepubertal, young adult, middle aged and old mice.

All previous studies on the turnover of AGEs have been carried out using AGE-proteins tagged with ^{125}I in the protein part. When ^{125}I-AGE-proteins are subjected to lysosomal proteolysis, the radioactive tag is rapidly released and disappears from the site of uptake, leaving the remaining parts undetectable. In addition, the short half-life of ^{125}I makes long-term studies impossible. To keep track of the AGEs during the entire degradation process following endocytosis, a stabile tagging of the AGE-adduct proper was developed. Using this tracer facilitated the observation that the ability of the liver scavenger cells to dispose of AGEs declined markedly after puberty, and then changed little up to high age.

2. Materials and methods

2.1. Reagents

Collagenase-P and protease inhibitors were from Roche Diagnostics GmbH. Fatty acid free BSA (99% purity), and RPMI-1640 medium were from Sigma. Percoll, and D-(U-^{14}C)-Glucose 323mCi/mmol were from Amersham–Pharmacia Biotech. Tissue solubilizer "Solvable" and "Ultima Gold" scintillation cocktail were from PerkinElmer.

2.2. Animals

Male C57Bl/6J mice, 14 and 28 months old, were purchased from Aged Rodent Colonies, National Institute on Aging (NIA), USA. C57Bl/6J mice, 3 months old were from Charles River Laboratories. Pre-pubertal (0.8 months old) males were obtained by breeding C57Bl/6J mice from Charles River Laboratories. In the hepatocellular

distribution study, 0.8 months and 3 months old C57BL/6N males from Harlan were used. Prior to ligand administration, the mice were anaesthetized with fentanyl and fluanizon (Hypnorm™, Janssen Pharmaceutical), in combination with midazolam (Dormicum™, Roche). The study was approved by the Norwegian Ethics Committee for Research on Animals.

Four age groups of animals were chosen for the study: pre-pubertal (0.8 months old), young-adult (3 months old), middle-age (14 months old) and old (28 months old), corresponding to 9, 25, 50, and 80 years of human age respectively (Supplementary Fig.1).

2.3. Ligand Preparation

BSA (50mg/ml) was incubated with 75mM ^{14}C-glucose in 0.33M disodium hydrogen phosphate/NaOH buffer (pH11) for two weeks at 50˚C. The total volume of the incubation mixture was 42μl. Non-incorporated ^{14}C-glucose was removed by size exclusion chromatography on Superdex-70 column (Amersham–Pharmacia Biotech). The resulting ^{14}C-AGE-BSA carried specific radioactivity (420000dpm/μg) sufficient for long term tracking of intracellular metabolism of the AGE-adduct.

Following intravenous injection of ^{14}C-AGE-BSA, the rate of blood clearance was found to be similar to what was reported for ^{125}I-AGE-BSA (Smedsrod et al., 1997; Svistounov et al., 2003), with all injected radioactivity eliminated from circulation within 5min (Supplementary Fig.2).

2.4. Anatomical Distribution of ^{14}C-AGE-BSA

^{14}C-AGE-BSA (4.7μg, 2x10^{6}dpm) was injected into the tail vein of anaesthetized pre-pubertal (n=9), young-adult (n=6) and old mice (n=7) via catheter allowing precise

administration. Animals were killed at 1.5h, 24h, 1, 2, 3, 4, 5, or 8 weeks after injection. Organs were extirpated, solubilized in "Solvable" and their radioactivity measured in a Packard Liquid Scintillation Counter using "Ultima Gold".

In a preliminary study performed in young-adult (n=3), middle-aged (n=3) and old mice (n=1) at 1.5h, 24h and 1 week after injection, carcasses without internal organs were found to contain 11% of total recovered radioactivity without any difference between the age groups or the time points after ligand administration, while internal organs contained 89% of the radioactivity. Radioactivity in the carcasses was quantified by combustion analysis in a Packard Sample Oxidizer.

2.5. ^{14}C-AGE-BSA Hepatic Disposal

Pre-pubertal (n=28), young-adult (n=27), middle-aged (n=29) and old mice (n=23) were injected with ^{14}C-AGE-BSA (4.7μg, 2x10^{6}dpm) as described above. The livers were collected at 1.5, 6, 12, 24, 48 h and 0.5, 1, 1.5, 2, 3.5, 5, 8 and 12 weeks after injection. Up to six animals were killed at each time point per age group for measurement of liver radioactivity.

2.6. Hepatocellular Distribution of ^{14}C-AGE-BSA

Animals from pre-pubertal and young-adult groups were injected with ^{14}C-AGE-BSA (9.4μg/animal) via a catheter into the tail vein, and killed 10min or 4 weeks post-injection. PCs, KCs and LSECs were isolated(Hansen et al., 2002; Smedsrod and Pertoft, 1985) and maintained in RPMI-1640 for 1h prior to assessment of cell numbers (average cell counts from 13 random 0.04 mm^2 squares per culture). The cultured cells were then

solubilized for radioactivity measurement.

2.7. Subcellular Fractionation

Five weeks after ^{14}C-AGE-BSA injection, livers of terminally anaesthetized, overnight-fasted mice were perfused with ice-cold buffer until bloodless, excised and homogenized by mild mechanical force in Dounce homogenizer (Bellco Glass) in 0.25M sucrose containing 20mM Hepes pH 7.4, 10mM EDTA and protease inhibitors. The post-nuclear supernatants were centrifuged through linear sucrose gradient (21-54% W/W) for 5h at 85000g followed by fraction collection. All the steps were carried out at 4˚C. Fraction densities were calculated from refractive indices (Rickwood and Graham, 1997). Radioactivity and activity of acid DNAse ((a lysosomal marker) (Wattiaux et al., 1993)) were assayed in fraction aliquots.

2.8. Size Exclusion Chromatography

Animals were placed in metabolic cages for a 12h period up to 5 weeks after ^{14}C-AGE-BSA injection. Collected urine was stored at -70˚C. Size distribution of urinary ^{14}C-AGE-DPs collected at 1, 2, 6, 18, 29 and 36 days after injection, was analysed using DIONEX HPLC system with “Superdex-Peptide” column (GE Healthcare) and “Radioactivity flow detector for HPLC LB 509” (BERTHOLD TECHNOLOGIES). Molecular weights of the ^{14}C-AGE-DPs were calculated from the standard curve generated by plotting the retention time of the manufacturer recommended standards against their corresponding molecular weights.

2.9. Data Analysis

The liver ^{14}C-AGE-associated radioactivity (expressed as % dose) versus time data were analyzed using non-linear regression (Prism-4, GraphPad Software). The model that best described the radioactivity disposal data was selected using the Akaike's Information Criterion (AIC) (Fig.2). The differences between age groups were determined by comparing best-fit values of parameters such as C and half-life using the F-test (Tab.1). The hepatocellular distribution of ^{14}C-AGEs data was analyzed by one–way ANOVA and Tukey HSD posthoc tests, using the SPSS software (Fig.3).

3. Results

3.1. Ligand Preparation

Tagging of AGE with ^{125}I in the protein moiety has the serious disadvantage that the tracer is rapidly lost when the protein moiety is subjected to endo/lysosomal proteolysis, leaving the AGE-adducts undetectable. We developed a microscale method for incorporation of ^{14}C in AGE-adducts based on published techniques (He et al., 1999), but with improved glucose to protein conjugation. The resulting ^{14}C-AGE-BSA allowed for the first time studies on the intracellular metabolism of the AGE-adduct proper.

3.2. Anatomical Distribution of Intravenously Administered ^{14}C-AGE-BSA

The organ distribution of intravenously injected ^{14}C-AGE-BSA was measured in pre-pubertal, young-adult, and old mice at 1.5h, 24h, 1 week and at 3-5 time points up to 8 weeks after injection. More than 90% of the total recovered radioactivity was liver associated, irrespective of age and time after injection (Fig.1). A previous study similarly showed that most of the injected AGE-BSA labelled with ^{125}I in the protein part

distributed in liver of young mice (Svistounov et al., 2003).

3.3. Hepatic Disposal of ^{14}C-AGE

The most striking finding was that the overall rate of ^{14}C-AGE removal from the liver was markedly faster in pre-pubertal than in older individuals (Fig.2). Moreover, ^{14}C-AGE degradation products (^{14}C-AGE-DPs) were stored for months in the liver. There was also a slowdown in the early stage of ^{14}C-AGE disposal in old age (Fig.2-insert).
Applying non-linear regression analysis of the clearance data in Fig.2 allowed the following interpretations (Tab.1): i) a three-phase exponential decay model provided the best description of liver radioactivity-time relationship for pre-pubertal, young-adult and middle-age groups (99% probability), whereas a two-phase exponential decay model fitted the old group with 97% probability (AIC test). ii) Removal of ^{14}C-AGEs from the liver proceeded through three phases: initial (fastest), intermediate and terminal (slowest) in all groups except the oldest. iii) A substantial proportion of radioactivity was removed during the initial phase (C_1 Tab.1). Rapid removal rates made the total exposure of livers to AGEs very low during this phase as reflected by area under the curve (AUC_1 Tab.1). This phase was not observed in the old-age group. iv) Most of the ^{14}C-AGE-DPs were removed during the intermediate phase (C_2 Tab.1). Relatively rapid removal made the exposure to ^{14}C-AGE-DPs moderate in this phase except for the pre-pubertal group where exposure was highest in the intermediate phase (AUC_2 Tab.1). v) Although the lowest proportion of radioactivity was removed during the terminal phase (C_3 Tab.1), the very slow removal in all post-pubertal groups (half-life$_3$ Tab.1) resulted in the highest exposure to the ^{14}C-AGE-AGEs in this phase (AUC_3 Tab.1). vi) In the pre-pubertal animals the

lowest proportion of ^{14}C-AGE-DPs, disposed of through the terminal phase (C_3 Tab.1) in combination with its relatively short half-life (half-life$_3$ Tab.1), resulted in a markedly lower exposure of livers to AGE-DPs compared with other groups during the terminal phase (AUC_3 Tab.1) and even to the intermediate phase in the same group (AUC_2 Tab.1). vii) The proportion removed during the terminal phase increased markedly with age (C_3 Tab.1). The changes in removal rate in this phase resembled the pattern observed for the intermediate phase (C_2 Tab.1).

3.4. Hepatocellular Distribution of ^{14}C-AGE

The greatest age-related difference in the rate of disposal of ^{14}C-AGEs from liver occurred between the pre-pubertal and young-adult mouse groups (Fig. 2). We therefore performed hepatocellular distribution studies in these two age groups. PC, KC and LSEC cultures were prepared 10 min and 4 weeks after intravenous injection of ^{14}C-AGE-BSA in pre-pubertal and young-adult mice. In both age groups, and at both time points, most of the radioactivity was located in LSECs and KCs (Fig. 3A, B), with very little radioactivity in PCs.

Ten minutes after ligand injection, the radioactivity per LSEC was higher in pre-pubertal animals, probably reflecting fewer LSECs than in young-adult mice due to smaller liver size, whereas no difference in radioactivity per KC was detected (Fig.3A).

At 4 weeks post-injection the remaining radioactivity per LSEC and KC was significantly higher in the young-adult than in the pre-pubertal groups (Fig.3B), supporting the observation of fastest AGE-DPs removal in the pre-pubertal group. The results further show that the cell efficacy to eliminate AGE-DPs after uptake decreases both in LSECs and KCs after puberty.

3.5. Subcellular Localisation of ^{14}C-AGE

All radioactive material in the gradients originated from KCs and LSECs. At the same time only about 50% of acid DNAse was derived from KCs and LSECs while the rest originated from PC (Wattiaux et al., 1993). Lysosomes from all three cell types normally band at the same density on sucrose gradient (Wattiaux et al., 1993).

Subcellular fractionation of liver homogenates at 5 weeks post-injection revealed radioactivity peaks banding at virtually the same sucrose gradient density in all the age groups (Fig.4A-D). The lysosomal marker acid DNAse banded at a markedly lower density compared with the position of the radioactivity peak in pre-pubertal group (Fig.4A). With age, the banded density of acid DNAse gradually shifted towards higher density (Fig.4B-C). In the old-age group, the acid DNAse peak co-eluted with the radioactivity peak (Fig.4D).

3.6. Size Distribution of Urinary ^{14}C-AGE-DPs

Size fractionation of urine samples was performed at 1, 2, 6 and 18 days after ^{14}C-AGE-BSA injection to analyze the AGE-DPs (Fig. 5). Radioactive material started eluting at retention time 53min, corresponding to 12900Da. However, very little material eluted in this region. The typical peak width for the "Superdex-Peptide 10/300 GL" column is 5-6 min at flow rate 0.2ml/min. Therefore, the detected radioactive peaks represented elution of heterogeneous material with overlapping molecular size.

Low MW ^{14}C-AGE-DPs (140-1650Da at "Full width at half maximum" (FWHM)) prevailed in the urine samples on day 1 post-injection but pre-pubertal mice exhibited a broader MW spectrum of excreted material versus the other age groups (70-2370Da at

FWHM, Fig.5A). With time, the MW profile of ^{14}C-AGE-DPs in urine became broader due to gradual shifting towards a higher MW region (FWHM 210-3700Da at day 18), but this shift was more pronounced in the pre-pubertal group (FWHM 260-5410Da at day 18). Nevertheless, at day 29 post-injection, the MW of ^{14}C-AGE-DPs from post-pubertal groups caught up with the pre-pubertal group and the elution profile remained the same until day 36 post-injection (not shown). The disappearance of the size difference between age groups in urinary ^{14}C-AGE-DPs at 4weeks post-injection can be due to initial and intermediate removal phases ending by this time.

At day 2 post-injection, there was retardation of the shift towards a higher MW region in the old-age group (Fig.5B).

4. Discussion

The present study demonstrates a profound difference in the overall rate of hepatic disposal of AGE-DPs between pre-pubertal and all post-pubertal age-groups, with a much faster AGE-DP elimination in the pre-pubertal animals, and with only minor differences between young-adult, middle-age and old mice. Moreover, senescence is associated with disappearance of the initial fast phase of AGE-DP disposal.

There is a clear difference in the fate of the protein and carbohydrate derived part of AGE. The half-life of the protein component of ^{125}I-AGE-BSA internalized by the liver is only a few minutes as judged by the speed of release of ^{125}I which tags the protein part of AGE (Svistounov et al., 2003). Although degradation is markedly slower in vitro than in vivo, more than 50% of ^{125}I-AGE-BSA is degraded and released by cultured LSECs already 5-6 h after exposure to the ligand (Smedsrod et al., 1997), whereas, in the present

study, a time period of 17 to 48 h was required for the liver to dispose of 50% of the sequestered ^{14}C-AGE-BSA labelled with ^{14}C in the AGE part. Thus, using ^{14}C-AGE-BSA of high specific radioactivity, we show for the first time that the AGE moiety proper is stored in the scavenger cells for a much longer time than the protein moiety.

At 12 weeks post-injection 3.2, 2.8, and 2.1% of the administered ^{14}C-AGE is still left in livers of young-adult, middle-age, and old mice, compared to only 0.31% (technically complete removal) in pre-pubertal livers. It can be extrapolated that it would take 29, 32 and 21 weeks to remove AGE-DPs to the level of the pre-pubertal group for the adult, middle-age and old-age groups respectively, (corresponding to 27, 30 and 20 years of human age (Supplemental Fig.1)). This remarkably prolonged intralysosomal persistence of AGE-DPs is due to a very slow terminal disposal phase which is responsible for most of the total exposure of liver scavenger cells to AGE-DPs in young-adult, middle-age and old groups, whereas in the pre-pubertal group this exposure is 6.5; 4.9 and 7.4 times lower, respectively.

The distribution of radioactivity on the gradient reflects the distribution of ^{14}C-AGE-DPs in KCs and LSECs whereas the distribution of acid DNAse reflects the distribution of lysosomes in both KCs, LSECs and PCs. Although the specific activity of this enzyme is 18 and 13-fold higher in LSECs and KCs respectively compared to PCs (De Leeuw et al., 1990), the overall ratio of acid DNAse originating from PCs and sinusoidal cells is approximately 50/50 (Wattiaux et al., 1993) because the PCs outmass other cell types in liver.

In all age groups ^{14}C-AGE derived radioactivity bands at the typical density for liver

lysosomes on sucrose gradients (1.2-1.24g/ml) (1997; Wattiaux et al., 1993). Acid DNAse peaks in the typical lysosomal region only in post-pubertal groups. It has been claimed that lysosomes from hepatocytes and sinusoidal cells can not be distinguished by sucrose density gradient (Wattiaux et al., 1993). However, until now the lysosomal density has been studied only in cells from mature animals (1997; Wattiaux et al., 1993), and a possible lysosomal density shift in PCs and/or sinusoidal cells at very young age can not be ruled out. A lower density of lysosomes at this age could explain the observed phenomenon.

A gradual increase in the density of the acid DNAse peak results in its co-elution with the radioactivity peak at old-age. The higher density of the radioactivity peak compared with the lysosomal marker peak in the younger animals can also be explained by tracer localisation in different subclasses of lysosomes. Breakdown of poorly degradable material takes place in late or terminal lysosomes (Kjeken et al., 1995). Incomplete digestion causes undigested material to accumulate and generate residual bodies, also called tertiary lysosomes, or dense bodies (Nixon and Cataldo, 1993; Schmucker and Sachs, 2002) that are denser than lysosomes (Roederer et al., 1989; Rome et al., 1979). Presumably at 5 weeks post-injection the remaining ^{14}C-AGE-DP concentrates in the terminal part of the endosomal-lysosomal route i.e. in residual bodies. Gradual age-related shifts of acid DNase to a higher density region could reflect increased proportion of residual bodies with age. The latter has been reported in hepatocytes, LSECs and KCs (de Leeuw et al., 1983; De Leeuw et al., 1990; De Priester et al., 1984; Schmucker and Sachs, 2002). Residual bodies also increase in diabetes when AGEs formation is accelerated (Giacomelli et al., 1980).

Analysis of the hepatocellular distribution of administered ^{14}C-AGE-BSA revealed that the ligand is taken up exclusively in the KCs and LSECs, the latter representing specialized scavenger endothelial cells with extraordinarily high pinocytic activity (Sorensen et al.). Interestingly, both cell types show decreased efficiency of ^{14}C-AGE-DP elimination after puberty, suggesting that the post-pubertal decline in disposition of AGE-DPs reflects a systemic age-related change.

Blood concentration of ^{14}C-AGE-DPs is very low (Fig.1) indicating their rapid kidney clearance. Thus, changes in the MW profile of urinary ^{14}C-AGE-DPs reflect liver rather than kidney function. Very low MW ^{14}C-AGE-DPs dominate in the urine soon after injection. With time, the proportion of higher MW ^{14}C-AGE-DPs in the urine increases. This indicates that predominantly low MW ^{14}C-AGE-DPs are excreted during the initial disposal phase whereas higher MW material is processed during the intermediate and terminal phases. Twenty-one known AGEs in free form, ranging from 220Da (carboxy methyl lysine; CML) to 545Da (Crosslines)(Ling et al., 1998; Niwa, 2006). Therefore, most of the urinary ^{14}C-AGE-DPs at day 1 (Fig.5A) should be free-AGEs, whereas the majority of ^{14}C-AGE-DPs appearing later consists of ^{14}C-AGE-peptides.

Pre-pubertal animals exhibit an increased ability to excrete very low and intermediate MW AGE-DPs. Note the broader MW spectrum (day1) and higher MW spectrum (days5 and 18) in the pre-pubertal mice vs. other age groups. This is in accordance with the observation of increased proportion of AGE-DPs being removed in the fast phase and faster removal rate in intermediate and slow phases in the pre-pubertal group. The shift of

urinary ^{14}C-AGE-DPs towards higher MW is delayed at day 2 in the old-age group (Fig.5B), reflecting the absence of an initial removal phase in this group (Fig.2-insert and Tab.1).

AGE-modified proteins are resistant to proteases (Miyata et al., 1997; Sell et al., 1996), which could account for the slow removal of ^{14}C-AGE-BSA associated radioactivity from liver. It may be postulated that the different age-related abilities to discharge AGE-DPs reside in different levels of lysosomal enzymes in hepatic scavenger cells from pre- and postpubertal individuals. However, specific activities of most lysosomal enzymes are unchanged or increased with age in LSECs, KCs or PCs (de Leeuw et al., 1983; De Leeuw et al., 1990; De Priester et al., 1984; Zhang and Cuervo, 2008). *In vitro* generated AGEs are highly aggregated (Svistounov et al., 2003). However, as early as 24h post-injection most radioactivity is associated with low MW material (SDS-PAGE of liver homogenates, not shown). This suggests that the liver scavenger cells are capable of degrading AGE-proteins but encounter problems with the excretion of AGE-DPs.

It is unknown how AGE-DPs leave the scavenger cells after uptake. Theoretically, free-AGEs and AGE-peptides of various size may find their way out of the lysosomes and cells by means of i) membrane transporters (present in both lysosomal end plasma membranes) (Forster and Lloyd, 1988); ii) free diffusion (Forster and Lloyd, 1988; Iveson et al., 1989), iii) retrograde transport along the endocytic pathway (Aniento et al., 1993; Jahraus et al., 1994), or iv) lysosomal exocytosis (Tam et al.). When discussing the mechanism of how AGE-DPs are discharged from the liver scavenger cells, one should bear in mind that most – if not all - such studies have been carried out as short term (minutes – hours) experiments with cells or organelles in vitro, whereas in the present

study the time scale is much greater (days-weeks), and takes place in the intact animal. Therefore, even low efficiency mechanisms such as free diffusion may be important. Nevertheless, the process termed lysosomal exocytosis, which has been shown to be a general pathway for cells to rid themselves of undegradable lysosomal waste contents (De Bruyn and Cho, 1986; Medina et al.; Tam et al.), appears as a likely exodus path for these non-degradable AGE-DPs.

Since young-adult mice cannot be considered as aged, the marked decrease in the rate of AGE-DPs removal in these mice, compared with pre-pubertal animals can hardly be explained by age-related deterioration of this function. Therefore, the decline in AGE-DPs removal rate in the young-adult group is likely to be a consequence of a physiological process but may in turn lead to waste accumulation and aging.

In summary:

Disposal of endocytosed AGE-DPs from the liver is a slow process. Elimination of these adducts from liver scavenger cells in mice is fastest in pre-pubertal animals and decreases significantly after sexual maturation. No major age-related changes are observed in the efficiency of liver disposal of AGEs from young-adult to middle-aged mice. However, senescence is associated with disappearance of the initial liver disposal phase.

Acknowledgments

The work was supported by the National Institute of Health (NIH), USA, (grant no. 1.R21AG026582-01A1); the Norwegian Research Council (grant no. 153483/V50); the Tromsø Research Foundation; and the Basque Government, Spain (grant no. BFI 05.525).

References

Baynes, J.W., Thorpe, S.R., 1999. Role of oxidative stress in diabetic complications: a new perspective on an old paradigm. Diabetes 48, 1-9.

Horie, K., Miyata, T., Yasuda, T., Takeda, A., Yasuda, Y., Maeda, K., Sobue, G., Kurokawa, K., 1997. Immunohistochemical localization of advanced glycation end products, pentosidine, and carboxymethyllysine in lipofuscin pigments of Alzheimer's disease and aged neurons. Biochem Biophys Res Commun 236, 327-32.

Ling, X., Sakashita, N., Takeya, M., Nagai, R., Horiuchi, S., Takahashi, K., 1998. Immunohistochemical distribution and subcellular localization of three distinct specific molecular structures of advanced glycation end products in human tissues. Lab Invest 78, 1591-606.

Miyata, S., Liu, B.F., Shoda, H., Ohara, T., Yamada, H., Suzuki, K., Kasuga, M., 1997. Accumulation of pyrraline-modified albumin in phagocytes due to reduced degradation by lysosomal enzymes. J Biol Chem 272, 4037-42.

Sell, D.R., Lane, M.A., Johnson, W.A., Masoro, E.J., Mock, O.B., Reiser, K.M., Fogarty, J.F., Cutler, R.G., Ingram, D.K., Roth, G.S., Monnier, V.M., 1996. Longevity and the genetic determination of collagen glycoxidation kinetics in mammalian senescence. Proc Natl Acad Sci U S A 93, 485-90.

Makita, Z., Bucala, R., Rayfield, E.J., Friedman, E.A., Kaufman, A.M., Korbet, S.M., Barth, R.H., Winston, J.A., Fuh, H., Manogue, K.R., et al., 1994. Reactive glycosylation endproducts in diabetic uraemia and treatment of renal failure. Lancet 343, 1519-22.

Hammes, H.P., Hoerauf, H., Alt, A., Schleicher, E., Clausen, J.T., Bretzel, R.G., Laqua, H., 1999. N(epsilon)(carboxymethyl)lysin and the AGE receptor RAGE colocalize in age-related macular degeneration. Invest Ophthalmol Vis Sci 40, 1855-9.

Niwa, T., 2006. Mass spectrometry for the study of protein glycation in disease. Mass Spectrom Rev 25, 713-23.

Dunn, J.A., McCance, D.R., Thorpe, S.R., Lyons, T.J., Baynes, J.W., 1991. Age-dependent accumulation of N epsilon-(carboxymethyl)lysine and N epsilon-(carboxymethyl)hydroxylysine in human skin collagen. Biochemistry 30, 1205-10.

Schleicher, E.D., Wagner, E., Nerlich, A.G., 1997. Increased accumulation of the glycoxidation product N(epsilon)-(carboxymethyl)lysine in human tissues in diabetes and aging. J Clin Invest 99, 457-68.

Sell, D.R., Monnier, V.M., 1997. Age-related association of tail tendon break time with tissue pentosidine in DBA/2 vs C57BL/6 mice: the effect of dietary restriction. J Gerontol A Biol Sci Med Sci 52, B277-84.

Smedsrod, B., Melkko, J., Araki, N., Sano, H., Horiuchi, S., 1997. Advanced glycation end products are eliminated by scavenger-receptor-mediated endocytosis in hepatic sinusoidal Kupffer and endothelial cells. Biochem J 322 (Pt 2), 567-73.

Svistounov, D.N., Berg, T.J., McCourt, P.A., Zykova, S.N., Elvevold, K.H., Nagai, R., Horiuchi, S., Smedsrod, B.H., 2003. Lack of recognition of Nepsilon-(carboxymethyl)lysine by the mouse liver reticulo-endothelial system: implications for pathophysiology. Biochem Biophys Res Commun 309, 786-91.

Hansen, B., Arteta, B., Smedsrod, B., 2002. The physiological scavenger receptor function of hepatic sinusoidal endothelial and Kupffer cells is independent of scavenger receptor class A type I and II. Mol Cell Biochem 240, 1-8.

Smedsrod, B., Pertoft, H., 1985. Preparation of pure hepatocytes and reticuloendothelial cells in high yield from a single rat liver by means of Percoll centrifugation and selective adherence. J Leukoc Biol 38, 213-30.

Rickwood, D., Graham, J.M., 1997. Subcellular fractionation : a practical approach, 1 ed. Oxford University Press, USA, Oxford.

Wattiaux, R., Gentinne, F., Jadot, M., Dubois, F., Wattiaux-De Coninck, S., 1993. Chloroquine allows to distinguish between hepatocyte lysosomes and sinusoidal cell lysosomes. Biochem Biophys Res Commun 190, 808-13.

He, C., Sabol, J., Mitsuhashi, T., Vlassara, H., 1999. Dietary glycotoxins: inhibition of reactive products by aminoguanidine facilitates renal clearance and reduces tissue sequestration. Diabetes 48, 1308-15.

De Leeuw, A.M., Brouwer, A., Knook, D.L., 1990. Sinusoidal endothelial cells of the liver: fine structure and function in relation to age. J Electron Microsc Tech 14, 218-36.

Kjeken, R., Brech, A., Lovdal, T., Roos, N., Berg, T., 1995. Involvement of early and late lysosomes in the degradation of mannosylated ligands by rat liver endothelial cells. Exp Cell Res 216, 290-8.

Nixon, R.A., Cataldo, A.M., 1993. The lysosomal system in neuronal cell death: a review. Ann N Y Acad Sci 679, 87-109.

Schmucker, D.L., Sachs, H., 2002. Quantifying dense bodies and lipofuscin during aging: a morphologist's perspective. Arch Gerontol Geriatr 34, 249-61.

Roederer, M., Mays, R.W., Murphy, R.F., 1989. Effect of confluence on endocytosis by 3T3 fibroblasts: increased rate of pinocytosis and accumulation of residual bodies. Eur J Cell Biol 48, 37-44.

Rome, L.H., Garvin, A.J., Allietta, M.M., Neufeld, E.F., 1979. Two species of lysosomal organelles in cultured human fibroblasts. Cell 17, 143-53.

de Leeuw, A.M., Brouwer, A., Barelds, R.J., Knook, D.L., 1983. Maintenance cultures of Kupffer cells isolated from rats of various ages: ultrastructure, enzyme cytochemistry, and endocytosis. Hepatology 3, 497-506.

De Priester, W., Van Manen, R., Knook, D.L., 1984. Lysosomal activity in the aging rat liver: II. Morphometry of acid phosphatase positive dense bodies. Mech Ageing Dev 26, 205-16.

Giacomelli, F., Skoza, L., Wiener, J., 1980. Lysosomal enzymes in experimental diabetic cardiomyopathy. Clin Biochem 13, 227-31.

Sorensen, K.K., McCourt, P., Berg, T., Crossley, C., Couteur, D.L., Wake, K., Smedsrod, B., The scavenger endothelial cell: a new player in homeostasis and immunity. Am J Physiol Regul Integr Comp Physiol 303, R1217-30.

Forster, S., Lloyd, J.B., 1988. Solute translocation across the mammalian lysosome membrane. Biochim Biophys Acta 947, 465-91.

Iveson, G.P., Bird, S.J., Lloyd, J.B., 1989. Passive diffusion of non-electrolytes across the lysosome membrane. Biochem J 261, 451-6.

Aniento, F., Emans, N., Griffiths, G., Gruenberg, J., 1993. Cytoplasmic dynein-dependent vesicular transport from early to late endosomes. J Cell Biol 123, 1373-87.

Jahraus, A., Storrie, B., Griffiths, G., Desjardins, M., 1994. Evidence for retrograde traffic between terminal lysosomes and the prelysosomal/late endosome compartment. J Cell Sci 107 (Pt 1), 145-57.

Tam, C., Idone, V., Devlin, C., Fernandes, M.C., Flannery, A., He, X., Schuchman, E., Tabas, I., Andrews, N.W., Exocytosis of acid sphingomyelinase by wounded cells promotes endocytosis and plasma membrane repair. J Cell Biol 189, 1027-38.

De Bruyn, P.P., Cho, Y., 1986. In vivo exocytosis of lysosomes by the endothelium of the venous sinuses of bone marrow and liver: visualization at normal and low body temperature. Am J Anat 177, 35-41.

Medina, D.L., Fraldi, A., Bouche, V., Annunziata, F., Mansueto, G., Spampanato, C., Puri, C., Pignata, A., Martina, J.A., Sardiello, M., Palmieri, M., Polishchuk, R., Puertollano, R., Ballabio, A., Transcriptional activation of lysosomal exocytosis promotes cellular clearance. Dev Cell 21, 421-30.

Supplementary data

This article contains supplementary information including supplementary experimental procedures, two supplementary figures and supplementary figure legends.

Table 1 Pharmacokinetic parameters of ^{14}C-AGE-BSA disposition from the liver of different age groups

C is the coefficient of exponential model representing the distance from starting place to the bottom on the Y axis (expressed in % of injected dose).

Half-life values are derived from the exponent of the model used to describe the data (expressed in weeks).

Area under the curve (AUC) for each part of the curve is calculated as the C divided by the exponent (C/k) and representing exposure of liver to injected ^{14}C-AGE-BSA (expressed in % of dose per weeks). Total AUC is calculated as the sum of the AUC for each phase.

Subscripts 1, 2 and 3 refer to the initial, intermediate and terminal phases respectively.

Superscript indicates significance ($p<0.05$) in F-test vs. corresponding groups: pre-pubertal (p), young-adult (a), middle-age (m) and old (o).

Phases	**Parameters**	**Pre-pubertal**	**Young-adult**	**Middle-age**	**Old-age**
Initial	C_1	34	26	30	Absent
	half-life$_1$	0.10	0.06	0.07	Absent
	AUC_1	5.0	2.3	3.0	Absent
Intermediate	C_2	34 $^{vs.\ o}$	36 $^{vs.\ o}$	36 $^{vs.\ o}$	48 $^{vs.\ p, a, m}$
	half-life$_2$	0.51 $^{vs.\ m}$	0.64 $^{vs.\ o}$	0.78 $^{vs.\ p, o}$	0.36 $^{vs.\ a, m}$
	AUC_2	25	33	41	25
Terminal	C_3	3 $^{vs.\ a, m, o}$	15 $^{vs.\ p, m, o}$	10 $^{vs.\ p, a, o}$	23 $^{vs.\ p, a, m}$
	half-life$_3$	3.28 $^{vs.\ a, m}$	5.23 $^{vs.\ p, o}$	6.31 $^{vs.\ p, o}$	3.34 $^{vs.\ a, m}$

AUC_3	14	91	68	103
AUC_{total}	44	126	111	128

Figure legends

Figure 1 Anatomical distribution of intravenously injected ^{14}C-AGE-BSA

Mice from pre-pubertal, young-adult and old age groups were injected with ^{14}C-AGE-BSA (4.7µg; 2x10^6dpm), and killed at 1.5h, 24h, 1, 2, 3, 4, 5, or 8 weeks after injection for analyses of anatomical distribution of radioactivity. Results represent percentages of organ-associated radioactivity from total radioactivity recovered in listed organs at a given time point. Radioactivity in stomach, and small and large intestines were measured together with organ contents. *Value for empty urinary bladder, **value for gallbladder with bile. Data represent mean values ± SD (n = 22 per organ). Since no significant difference in relative anatomical distribution of radioactivity was observed between either the age groups or the time points after ligand administration, pooled data were plotted in this figure.

Figure 2 ^{14}C-AGE hepatic disposal following uptake of injected ^{14}C-AGE-BSA

The fate of the ^{14}C-AGE tracer in the liver of pre-pubertal (green triangles), young-adult (red squares), middle age (yellow rings) and old (blue diamonds) mice was followed for 12 weeks after intravenous injection of ^{14}C-AGE-BSA (4.7 µg, 2×10^6 dpm). Radioactivity retained in liver is given as percentage of injected radioactivity (% dose) and is plotted in a semi-logarithmic plot (log2-linear scale) up to 12 weeks after injection.

The insert represents the linear plot (linear - linear scale) of the data up to 2 weeks after ligand administration. Mean ± SD shown ($n \leq 6$ per time point).

Each age group liver radioactivity–time profile was fitted to either 2-or 3-phase exponential models to describe the time course of liver radioactivity. These models have the mathematical form of

$A = C_1.e^{-k1*t}+C_2.e^{-k2*t}+C_3.e^{-k3*t}$ where A is the ^{14}C-AGE-associated radioactivity in liver (expressed as % dose), C is the coefficient from the exponential model, k is the exponent and t is time after injection (weeks). Half-life is calculated as ln2/k. The subscript 1, 2 and 3 refer to the initial, intermediate and terminal phases respectively. The AUC from each phase is calculated as C/k and the total AUC is the sum of the AUC for each phase. Curves are built from parameters obtained by fitting two-phase exponential decay (old group) and three phase exponential decay (pre-pubertal, young-adult, middle-aged groups) models to the data points. The model that best described the radioactivity disposal data was selected using the Akaike's Information Criterion (AIC).

Figure 3 Hepatocellular distribution of ^{14}C-AGEs in pre-pubertal and young-adult mice

Pre-pubertal and young-adult mice were injected intravenously with ^{14}C-AGE-BSA. The animals were euthanized after 10 min (A) or 4 weeks (B) and radioactivity (dpm/million cells) was measured in solubilized cultures of purified parenchymal cells (PC), Kupffer cells (KC), and liver sinusoidal endothelial cells (LSECs). AGE-BSA injection dose: 9.4 μg/animal; in the 10 min group this dose was achieved by mixing 2.35 μg ^{14}C-AGE-BSA

($1x10^6$ dpm) with 7.05 μg non-radioactive AGE-BSA, while the 4 week group was injected with 9.4 μg of ^{14}C-AGE-BSA ($4x10^6$ dpm).

A) Radioactivity[#] in liver cells 10 min after ligand injection in 0.8 month old (open bars, n=7) and 3 month old mice (filled bars, n=6). [#]Adjusted values.

B) Radioactivity in liver cells 4 weeks after ligand injection in 0.8 month old (open bars, n=6) and 3 month old mice (filled bars, n=8).

* Significant difference ($p<0.01$) in ^{14}C-radioactivity in corresponding cell types isolated from mice injected at 0.8 months and 3 months of age. Error bars: SD.

[#]In Fig. 3A (10 min group) dpm values measured in samples were multiplied by four to reflect the real difference in AGE content in liver cells isolated at 10 min and 4 weeks after injection.

Figure 4 Subcellular localization of ^{14}C-AGEs

^{14}C-AGE-BSA (4.7 μg, 2×10^6 dpm) was injected intravenously in pre-pubertal (A), young-adult (B), middle-aged (C) and old (D) mice. Livers were surgically extracted, homogenized , and cellular compartments were separated on linear sucrose gradient 5 weeks after ^{14}C-AGE-BSA injection. Radioactivity and acid DNAse (a lysosomal marker(De Leeuw et al., 1990)) activity were measured in the sucrose gradient fractions. Acid DNAse indicates the location of lysosomes on the gradient. About 50% of this enzyme come from KCs and LSECs and the rest originates from PCs (Wattiaux et al., 1993). Lysosomes from all three cell types normally banded at the same density on sucrose gradient (Wattiaux et al., 1993).

All radioactive material in the gradient originates from KCs and LSECs.

Results are presented as % of maximum detected radioactivity (squares, solid line) and % of maximum detected acid DNase activity (triangles, dashed line) in the fractions as a function of the gradient density.

A- pre-pubertal; B- young-adult; C- middle-age and D- old-age groups.

The radioactivity peak banded at virtually the same sucrose gradient density 1.223-1.229g/ml in all age groups (panels A-D). Acid DNAse peak banded at density 1.193; 1.202; 1.205 and 1.225g/ml in pre-pubertal; young-adult; middle-age and old-age groups respectively (panels A-D).

Figure 5 Size distribution of ^{14}C-AGE-DPs in urine

Urine samples were collected 1 day (A), 2 days (B), 6 days (C) and 18 days (D) after intravenous injection of ^{14}C-AGE-BSA (4.7 μg, 2×10^6 dpm, per animal).

Size distribution of urinary ^{14}C-AGE-DPs from pre-pubertal (n=4, green line), young-adult (n=2, red line), middle-aged (n=2, yellow line) and old (n=1, blue line) mice was performed by size exclusion chromatography using Superdex peptide 10/300 GL column. MW were calculated from the standard curve generated by plotting the retention time of protein standards against their corresponding MW Results presented are representative chromatograms of one animal per age group at the different time points.

The two x-axes represent MW distribution (Da, lower x-axis) and retention time (min, upper x-axis). Signal intensity is expressed as ^{14}C radioactivity (% of maximum detected) is plotted along the y-axis. V_o - void volume of the column; V_{tot} - total volume of the column.

Figures

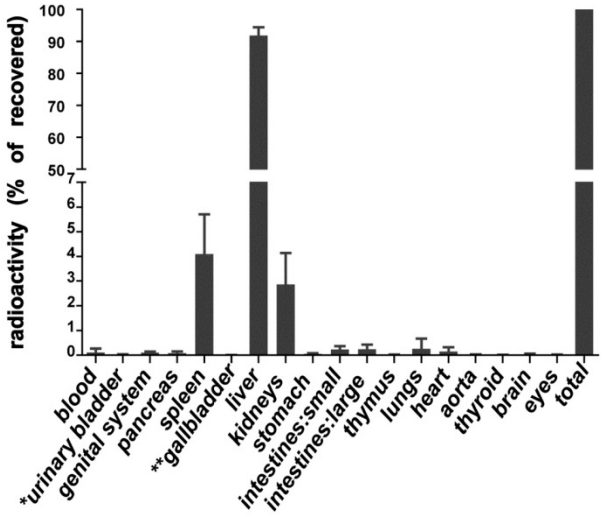

Figure 1 Anatomical distribution of intravenously injected ^{14}C-AGE-BSA

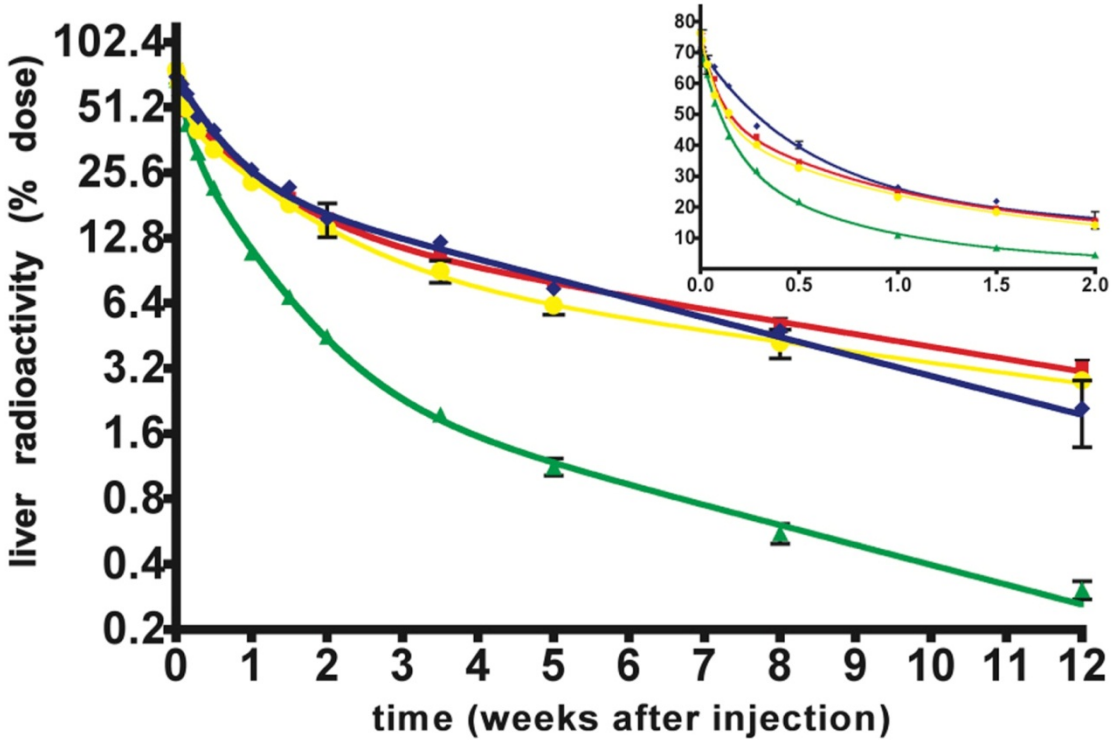

Figure 2 ^{14}C-AGE hepatic disposal following uptake of injected ^{14}C-AGE-BSA

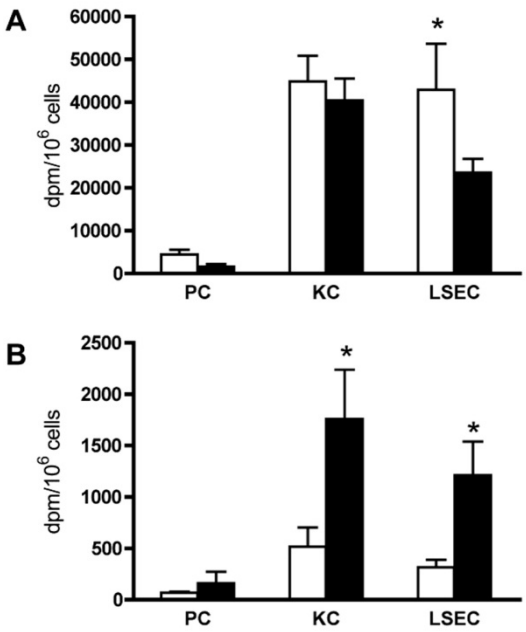

Figure 3 Hepatocellular distribution of ^{14}C-AGEs in pre-pubertal and young-adult mice

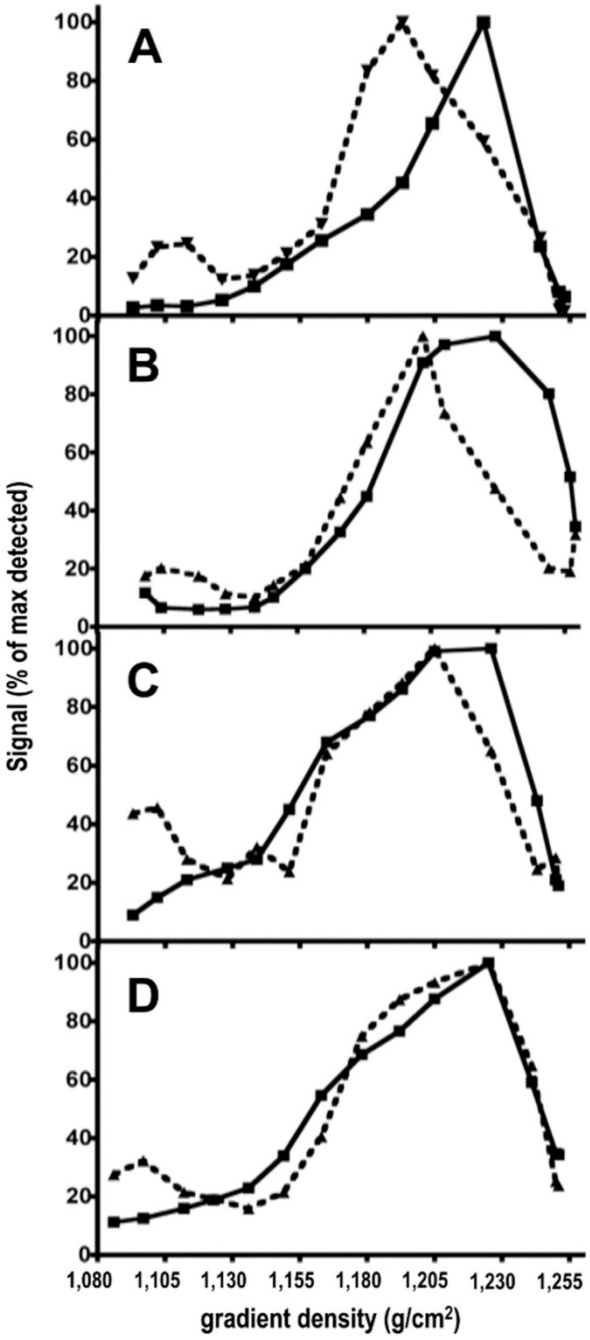

Figure 4 Subcellular localization of ^{14}C-AGEs

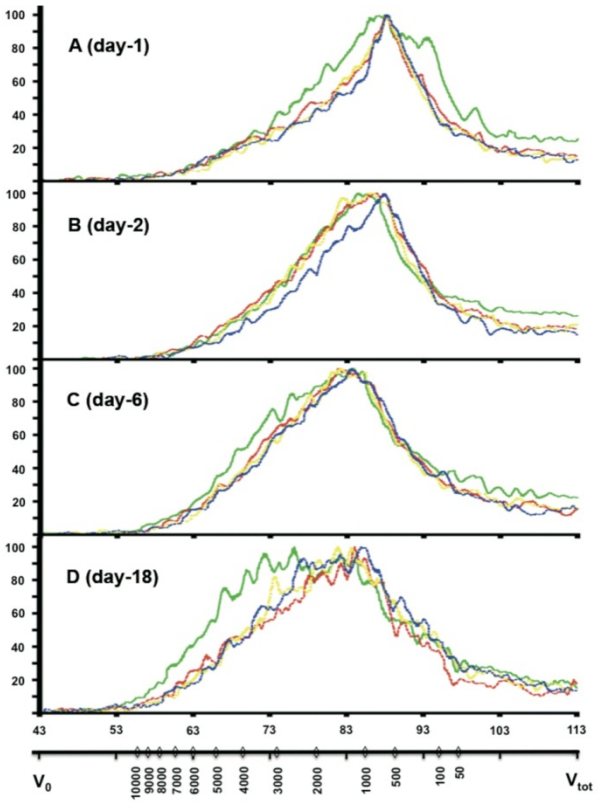

Figure 5 Size distribution of ^{14}C-AGE-DPs in urine